

Intramolecular Exciton Coupling and Induced Circular Dichroism From Bilirubin-Ephedrine Heteroassociation Complexes. Stereochemical Models for Protein Binding

*Yu-Ming Pu and David A. Lightner**

Department of Chemistry, University of Nevada, Reno, Nevada 89557-0020, USA

Received September 5, 1988

Bichromophoric (4Z,15Z)-bilirubin-IX α , the cytotoxic and yellow-orange pigment of jaundice, prefers to adopt either of two enantiomeric intramolecularly hydrogen-bonded conformations that are in dynamic equilibrium in solution. In the presence of optically active amino-alcohols, particularly ephedrines, the pigment solutions exhibit intense bisignate circular dichroism in the region of the bilirubin long wavelength UV-visible absorption band. The most intense circular dichroism Cotton effects, $|\Delta\epsilon| \rightarrow 200$, are induced by O-methylephedrines, exceeding even those generally exhibited by bilirubin complexes with serum albumin and other proteins. Like serum albumin and other proteins, the optically active amino alcohols act as chiral templates, inducing an asymmetric transformation of bilirubin, whose induced bisignate circular dichroism Cotton effect originate from exciton splitting of its two component pyrromethenone chromophores. The amines are thought to serve as agents for chiral molecular recognition by forming diastereomeric salts with the pigment. And the complementary action of β -aryl and proximal hydroxyl and methoxyl groups provides insight into the binding forces important in bilirubin-protein binding.

INTRODUCTION

(4Z,15Z)-Bilirubin-IX α (BR-IX), the hydrophobic and cytotoxic yellow-orange pigment of jaundice, is produced abundantly by heme catabolism in mammals and is transported as a heteroassociation complex with serum albumin to the liver for glucuronidation and excretion.^{1,2} When ready excretion of the pigment is hindered as in newborn babies with physiologic jaundice or in individuals with certain liver pathologies, albumin acts as a biologic buffer against bilirubin encephalopathy³ and associated neurologic dysfunction.² Its affinity for BR-IX, is rapid, reversible and strong ($K_A \approx 10^8 \text{ M}^{-1}$ for the primary binding site),⁴⁻⁶ and the 1:1 complex exhibits an unusually intense bisignate circular dichroism (CD) curve for the otherwise optically inactive bichromophoric pigment.^{4,7,8} This striking spectroscopic phenomenon

The abbreviations used are: Br-IX, (4Z,15Z)-bilirubin-IX α ; BR-IX DME (4Z,15Z)-bilirubin-IX dimethyl ester; MBR-XIII, (4Z,15Z)-mesobilirubin-XIII α ; MBR-IV, (4Z,15Z)-mesobilirubin-IV α ; XBR, xanthobilirubinic acid; CD, circular dichroism; ICD, induced circular dichroism; CE, Cotton effect.

provides a sensitive and important probe of complexation parameters, protein topography and pigment structure. Yet, despite nearly 20 years of investigations of the protein-induced optical activity of BR-IX, an accurate description of the binding site and pigment structure is still unresolved and controversial.⁴⁻¹²

The three-dimensional structure of BR-IX (Figure 1) has been revealed through X-ray crystallographic^{13,14} and solution NMR studies¹⁵ as one in which extensive *intra*-molecular hydrogen bonds link the polar carboxylic acid and lactam functionalities. As a consequence of intramolecular H-bonding, BR-IX is considerably less polar and more hydrophobic than other bile pigments which do not have propionic acid groups located at pyrrole carbons 8 and 12,^{1,3} e. g., the β , γ and δ isomers of bilirubin.¹⁶ In bile pigment metabolism, this difference is seen in the *inexcretability* of the α isomer (BR-IX) across either of the selective barriers, liver and kidney, into bile or urine respectively. In marked contrast, the β , γ and δ isomers cross the liver rapidly, without conjugation.¹⁷ By esterifying the BR-IX carboxyl groups with glucuronic acid, thereby effectively increasing its water solubility and excretability,^{2,4} nature circumvents this problem and thus detoxifies the pigment. Jaundice in newborn babies is typically due to an inactivated glucuronidation mechanism, leading to retention of neurotoxic bilirubin. Nowadays, the typical and convenient treatment is phototherapy with visible light.¹

The physiologic importance of serum albumin is well known. What is less well known is the nature of its binding site for BR-IX and the structure of the bound pigment.⁵ Complexation of the pigment with albumin produces spectral shifts in the UV-visible (UV) spectrum and an intense bisignate induced circular dichroism (ICD ($\Delta\epsilon_{407}^{\max} - 25$, $\Delta\epsilon_{460}^{\max} + 50$) for BR-IX complexes with human serum albumin, as compared with BR-IX alone in pH 7.3 aqueous buffer (UV $\lambda_{\max} \sim 440$ nm, ICD $\Delta\epsilon = 0$).^{7,8} The data were shown to be consistent with the human serum albumin (at pH 7.3) binding predominantly the right-handed chiral conformation (P, Figure 1) of folded, intramolecularly hydrogen bonded BR-IX mono or dianion. Salt linkages to the BR-IX carboxylate anion(s) appear to be important in binding to the protein. Jacobsen's studies¹⁸ point to the importance of the lysine-240 residue at the binding site, along with possible assistance from neighboring arginine, tyrosine and histidine nuclei.¹⁹ Other binding contributions appear to come from hydrogen bonding, $\pi-\pi$ interactions and hydrophobic interactions.⁵ Yet, specific details of binding and factors which induce chirality of the pigment have remained unclear. With the probability that amine residues might serve as key elements in the chiral induction of BR-IX at the albumin site, we initiated an exploration of the induced CD of BR-IX and related pigments induced by optically active amines. Preliminary studies showed that (1) even simplest optically active amines, e. g., 2-aminobutane, will induce circular dichroism in solutions of BR-IX,²⁰ (2) the magnitude of the induced optical activity is related to the relative concentration and the structure of the amine,^{20,21} and (3) β -aryl groups of the amine tend to induce intense CD. In the present work we show that aromatic groups, hydroxyl groups and subtle stereochemical factors in a series of diastereomeric ephedrine (amino alcohol) complexing agents can lead to profound differences in the ICD of BR-IX.

The studies provide insights into potential binding mechanisms and a rationale for and the origin of the intense bisignate ICD of the BR-IX complex with serum albumins.

RESULTS AND DISCUSSION

Induced Circular Dichroism (ICD)

The ICD spectra (Figure 2) of BR-IX in the presence of diastereomeric (+)-(2*R*)-methylamino-(1*S*)-1-phenylpropanol [(+)-ephedrine] and (−)-(2*R*)-methylamino-(1*R*)-1-phenylpropanol [(−)-*ψ*-ephedrine] show intense bisignate Cotton effects (CEs) characteristic of those seen for heteroassociation complexes of BR-IX with serum albumins,⁷ e. g., $\Delta\epsilon_{407}^{\max} = -26$, $\Delta\epsilon_{460}^{\max} = +49$ for (BR-IX) : (human serum albumin) = 1 : 2 at pH 7.3.⁸ Unlike the BR-IX · albumin complexes, the CD magnitudes depend on the amine : BR-IX molar ratio, with maximum values reaching a plateau near ratios of 1,000 : 1 and decreasing substantially at ratios approaching the 2 : 1 albumin : BR-IX molar ratio commonly employed (Tables I and II). The data undoubtedly reflect a smaller

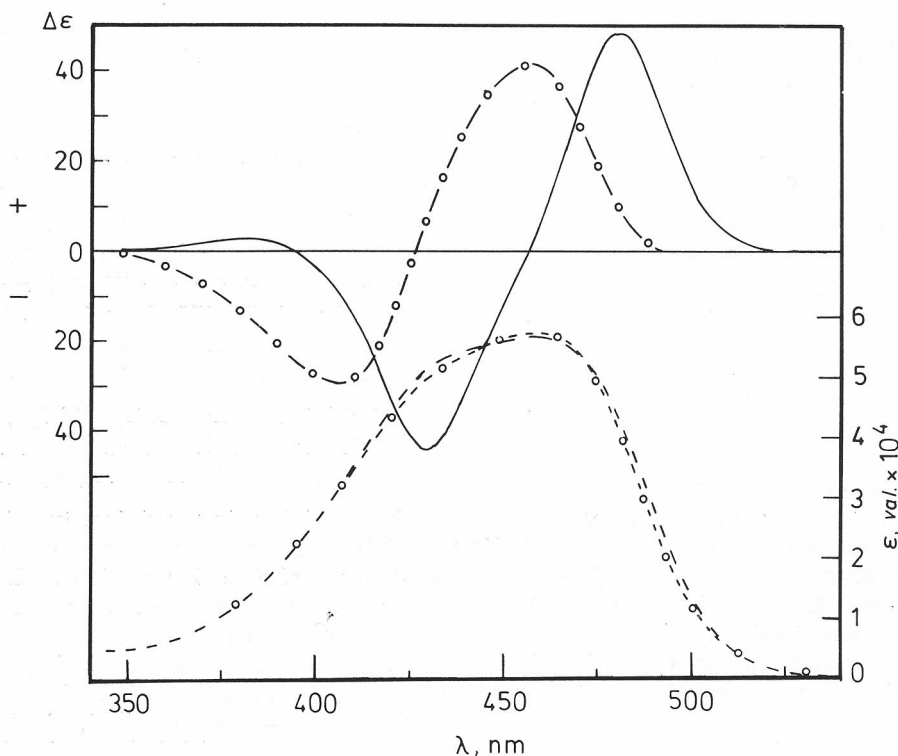


Figure 2. Circular dichroism (—) and UV-visible (---) spectra of 3.4×10^{-5} M bilirubin-IX α in ethanol-free chloroform (stabilized with cyclohexane) in the presence of 3.4×10^{-2} M (1*S*,2*R*)-(+)-ephedrine at 21 °C. Circular dichroism (○—○) and UV-visible (○---○) spectra of 3.4×10^{-5} M bilirubin-IX α in ethanol-free chloroform (stabilized with cyclohexane) in the presence of 3.4×10^{-2} M (1*R*, 2*R*)-(−)-*ψ*-ephedrine at 21 °C. The $\Delta\epsilon = 0$ line is the reference CD for BR-IX in the absence of the amine.

TABLE 1. Circular Dichroism (CD) and Ultraviolet-Visible (UV) Spectral Data for 3.4×10^{-5} M Bilirubin-IX α with Varying Concentrations of (1S,2R)-(+)-Ephedrine in Chloroform^a at 21°C.

(+) - Ephedrine: Bilirubin		CD			UV	
Molar Ratio	Time (h) ^b	$\Delta\epsilon_{\max}(\lambda_1)$	λ_2 at $\Delta\epsilon=0$	$\Delta\epsilon_{\max}(\lambda_3)$	ϵ_{\max}	(λ_{nm})
10:1	0.5	-5.2 (440)	472	+4.6 (490)	57,000	(452)
	24	-5.8 (435)	470	+4.1 (485)	57,400	(450)
100:1	0.5	-31.3 (435)	463	+30.5 (485)	56,000	(452)
	24	-30.5 (435)	464	+30.2 (485)	56,800	(452)
1,000:1	0.5	-58.6 (434)	462	+60.9 (485)	55,100	(456)
	24	-55.1 (435)	463	+56.8 (485)	52,100	(454)
5,000:1	0.5	-61.9 (437)	467	+60.1 (485)	53,700	(454)
	24	-54.7 (438)	467	+53.5 (490)	52,000	(454)

^a Ethanol-free, stabilized with 1% n-hexane.

^b Spectra run 0.5 hours and 24 hours after preparing solutions.

TABLE 2. Circular Dichroism (CD) and Ultraviolet-Visible (UV) Spectral Data for 3.4×10^{-5} M Bilirubin-IX α with Varying Concentrations of (1R,2R)-(-)- ψ -Ephedrine in Chloroform^a at 21°C.

(-)- ψ -Ephedrine: Bilirubin		CD			UV	
Molar Ratio	Time (h) ^b	$\Delta\epsilon_{\max}(\lambda_1)$	λ_2 at $\Delta\epsilon=0$	$\Delta\epsilon_{\max}(\lambda_3)$	ϵ_{\max}	(λ_{nm})
10:1	0.5	-1.50 (415)	435	+0.58 (460)	56,700	(452)
	24	-1.45 (415)	435	+0.58 (460)	57,000	(452)
100:1	0.5	-11.6 (410)	430	+14.5 (460)	56,370	(450)
	24	-9.28 (409)	431	+12.2 (460)	55,000	(451)
1,000:1	0.5	-37.4 (413)	433	+51.3 (465)	58,000	(450)
	24	-36.5 (410)	433	+49.6 (464)	56,900	(450)
5,000:1	0.5	-44.0 (413)	433	+60.9 (465)	57,600	(454)
	24	-44.4 (413)	434	+60.0 (465)	54,000	(454)

^a Ethanol-free, stabilized with 1% n-hexane.

^b Spectra run 0.5 hours and 24 hours after preparing solutions.

binding constant between BR-IX and the amino alcohols on one hand, and albumin on the other, where the extraordinarily tight binding ($K_A \approx 10^8 \text{ M}^{-1}$)⁴⁻⁶ rests on the considerable aqueous insolubility of BR-IX ($K_{\text{sol}} \approx 10^{-15} \text{ M}$)²² at physiologic pH. Since BR-IX is soluble in chloroform up to concentrations of $\sim 10^{-4} \text{ M}$, the ICD magnitudes of Tables I and II are all the more remarkable. And in comparing the data of Table I and II, it seems clear that (+)-ephedrine binds more tightly than (-)- ψ -ephedrine, for $|\Delta\epsilon|$ are appro-

ximately equal at the highest amino alcohol : pigment ratio but larger for (+)-ephedrine solutions at the lower ratios.

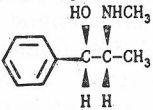
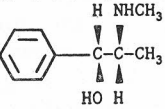
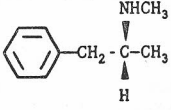
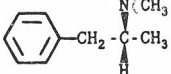
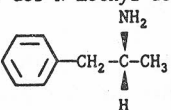
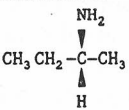
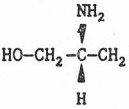
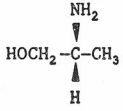
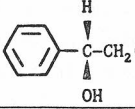
The Importance of the Chiral Complexation Agent Amino, Hydroxyl and β -Aryl Groups to ICD

Other amines and amino-alcohols can generate ICDs for BR-IX, as reflected in Table III, but none do it as well as the ephedrines, except desoxyephedrine and its N-methylated derivative. It may be noted that the β -phenylisopropylamine structure uniquely supports the largest CEs and that substantially weaker CD is induced by: (i) ephedrine analogs without phenyl groups, e. g., *R*-(—)-alaninol and *R*-(—)-2-aminobutanol and (ii) the desoxyephedrine or des-N-methyl-desoxyephedrine analogs without a phenyl group, e. g., *R*-(—)-2-aminobutane. These data would tend to indicate that the presence of a β -hydroxyl group is apparently much less important for inducing intense CD than a β -phenyl group, *cf.* the ephedrines and desoxyephedrine. However, the presence of an amino group is of fundamental importance, more important than either the aromatic group or the hydroxyl group as evidenced by the CD of *R*-(—)-phenyl-1,2-ethanediol. In fact, the CE magnitudes seen in Table III for ephedrine, ψ -ephedrine and desoxyephedrine approach the largest values ($\Delta\epsilon_{422}^{\max} + 129$, $\Delta\epsilon_{474}^{\max} - 208$) observed¹² for BR-IX complexes to human serum albumin (HSA) [(BR-IX) : (HSA) = 1 : 5, (BR-IX) = 2.5×10^{-5} M, pH 4.00] and exceed those recorded^{7,8} for BR-IX · HSA solutions near physiologic pH (*vide supra*). They contrast markedly with the considerably weaker CE magnitudes ($\Delta\epsilon_{460}^{\max} - 3.0$, $\Delta\epsilon_{409}^{\max} + 2.4$) for pH 8.0 BR-IX solutions with a 1000-fold molar excess of the chiral, toroid-shaped complexing agent,²⁵ α -cyclodextrin. The data clearly point to a complexation model in which amine salt formation plays a primary role, with cooperative effects coming from β -aryl and, apparently to a lesser extent, from β -hydroxyl groups in the chiral complexation agent.^{23,24} The stereochemistry of the hydroxyl group, *cf.* ICDs for BR-IX in the presence of (+)-ephedrine and (—)- ψ -ephedrine, does seem to affect the complexation process, but the stereochemistry at the chiral center bearing the amino functionality is clearly the dominant factor in determining the signed order of the CEs. And the extent to which the CEs can be perturbed by the location and stereochemistry of the neighboring OH group reflects on the possible importance of adjacent dipoles and H-bonding in the complexation. To understand the role of these binding elements in complexation, one must understand the chiral structures of bilirubin from which the CD originates.

Bilirubin Structure and the Origin of Induced Optical Activity

Bilirubin is capable of adopting a large number of chiral conformations, which have been mapped and evaluated by molecular orbital calculations.²⁶ These calculations and space-filled molecular models indicate that *Z*-configuration rubinoid pigments tend to adopt folded conformations (as in Figure 1.) as their low energy structures, even without invoking the readily accessible intramolecular hydrogen bonding. Thus, molecular mechanics calculations²⁷ reveal minimum energy conformations with essentially planar pyrromethenone units oriented by torsion angles $N_{22}-C_9-C_{10}-C_{11}$ and $C_9-C_{10}-C_{11}-N_{23}$ (Φ_1

TABLE 3. Circular Dichroism (CD) and Ultraviolet-Visible (UV) Spectral Data for $3.4 - 4.9 \times 10^{-5}$ M Chloroform Solutions of Bilirubin-IX α and 0.034-0.049 M Optically Active Amines^a at 20°C.

Amine	CD			UV	
	$\Delta\epsilon_{\max}(\lambda_1)$	λ_2 at $\Delta\epsilon=0$	$\Delta\epsilon_{\max}(\lambda_2)$	ϵ_{\max}	(λ_{nm})
(1S, 2R)-(+)-Ephedrine 	-58.6 (434)	462	+60.9 (485)	55,100	(456)
(1R, 2R)-(-)-ψ-Ephedrine 	-37.4 (413)	433	+51.3 (465)	58,000	(450)
R-(-)-desoxyephedrine 	-48.0 (418)	441	+62.5 (474)	58,200	(459)
R-(+)-N-Methyl-desoxyephedrine 	-85.3 (410)	434	+120.7 (462)	53,300	(448)
R-(-)-des-N-methyl-desoxyephedrine 	-12.0 (418)	438	+14.0 (474)	57,400	(462)
R-(-)-2-Aminobutane 	-6.5 (420)	440	+7.8 (474)	57,600	(455)
R-(-)-2-Aminobutanol 	-8.8 (415)	438	+12.2 (470)	58,400	(455)
R-(-)-Alaninol 	-2.8 (401)	427	+3.6 (458)	60,500	(460)
R-(-)-Phenyl-1,2-ethanediol 	-1.5 (405)	--	--	58,600	(457)

^a 1,000:1 amine:bilirubin molar ratio; CD and UV spectra run within 30 minutes of preparing solutions and exhibit little or no change when remeasured after 24 hours.

and Φ_2 , respectively) with values ranging from 60° to 120° . Intramolecular steric interactions tend to destabilize a wide spectrum of conformations, including the helical, skewed, extended and linear (Figure 3.). There are only a few shallow local minima on the energy hypersurface, and two deeper, global minima that correspond to the folded conformation of Figure 3. or its enantiomer.^{26,27} Intramolecular hydrogen bonding involving either the propionic acid, or its methyl ester, and an opposing pyrromethenone further lowers the energy of the folded conformations. For BR-IX, the folded, intramolecularly hydrogen-bonded (*»ridge-tile«*) conformers (Figure 1.) are calculated to be ~ 8.5 kcal/mole more stable than the corresponding folded (Figure 3.) conformers without hydrogen bonding.²⁶ Surprisingly perhaps, the folded, intramolecularly hydrogen-bonded conformers of the dimethyl ester of BR-IX, where only four hydrogen bonds are possible (between the carbomethoxy carbonyl oxygen and the lactam and pyrrole N—H groups), are calculated to be ~ 6 kcal/mole more stable than the corresponding folded conformer without hydrogen bonds.²⁶ Apparently even residual hydrogen bonding is a conformation-stabilizing force.

Experimental evidence confirms that BR-IX, both in the crystal^{13,14} and in non-polar solvents^{15,28} adopts the well-defined chiral secondary structures of Figure 1. and 3c. Even in polar solvents, such as DMSO, shiral conformations akin to those still predominate, with the propionic side chains coupled through solvent to their opposing pyrromethenone units. Using NMR, Navon and Kaplan^{15,28} have shown that in DMSO solution the segmental motion of the propionic side chains of BR-IX and its dimethyl ester is very limited, contrasting markedly with the independent fast motion of the propionic side chain of vinylneoxanthobilirubinic acid methyl ester, a mono-pyrromethenone model for one-half of bilirubin with its propionic group not involved in hydrogen bonding, except to solvent. The picture provided by Navon and Kaplan for BR-IX and BR-IX dimethyl ester is one where chiral conformations akin to those of Figure 1 still predominate, albeit with the propionic acid residues linked to the nearest lactam amide and pyrrole NH groups via bound solvent molecules. This view was reinforced recently by resonance Raman studies of BR-IX in DMSO.²⁹ In aqueous solutions of human serum albumin, BR-IX exhibited a different resonance Raman spectrum from that of its dianion (di-sodium salt). Interestingly, it showed a spectrum strongly resembling that of BR-IX in DMSO, for which NMR studies have concluded in favor of a folded conformation with solvent intervening in an intramolecular hydrogen bonding matrix.^{15,28} The Raman work adds to a consistent picture for this generalized model, although it cannot distinguish between the intrusion of water and the intrusion of NH_2 , OH, etc. functional groups of the protein residues into the hydrogen bonding matrix of the pigment. Additional support of this bonding model comes from the work of Mugnoli, Manitto and Monti,³⁰ who have shown that isopropylamine interferes with the BR-IX intramolecular hydrogen bonding matrix (Figure 1.) by (i) transferring the CO_2H proton to $-\text{NH}_2$ (salt formation) and (ii) donating all three $-\text{NH}_3^+$ protons back into the lactam carboxyl hydrogen bonding region of the folded pigment. Although the original hydrogen bonds of the *»ridge-tile«* structure are broken in the bis-ammonium salt, new and different hydro-

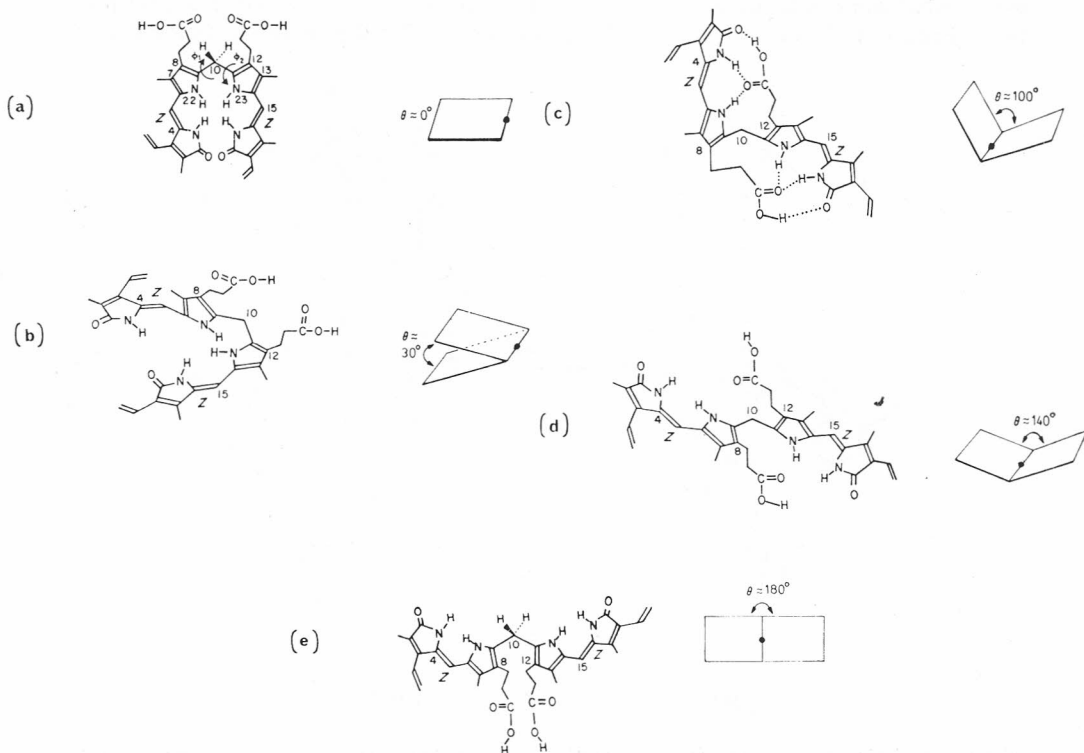


Figure 3. Conformational drawing of representative three-dimensional structures of (4Z,15Z)-bilirubin-IXa (BR-IX). The indicated BR-IX conformations are produced by rotations of the pyrromethenones in propeller fashion about the torsion angles Φ_1 and Φ_2 , corresponding to $N_{22}-C_9-C_{10}-C_{11}$ and $C_9-C_{10}-C_{11}-N_{23}$ respectively, while keeping the pyrromethenone units planar, i. e., torsion angles $C_4-C_5-C_6-N_{22}$ and $N_{23}-C_{14}-C_{15}-C_{16} \approx 0^\circ$. The dihedral angle (θ) corresponding to the intersection of the pyrromethenone planes is shown at the right of each structure, with the line of intersection passing through C_{10} , where C_{10} is represented by ●. (a) The $\theta \approx 0^\circ$ conformation is planar and «helical», with both pyrromethenones lying essentially in the same plane and $\Phi_1 \approx \Phi_2 \approx 0^\circ$. This conformation is porphyrin-like, but it has considerable steric hindrance associated, *inter alia*, with overlapping lactam centers. (b) The $\theta \approx 30^\circ$ conformation is skewed and helical with $\Phi_1 \approx \Phi_2 \approx 10-20^\circ$. It has a lock-washer-like shape and is shown with the plus (P) chirality. (c) Folded, «ridge-tile» conformations with $\theta \approx 90-110^\circ$ and $\Phi_2 \approx \Phi_1 \approx 60-70^\circ$. (d) The extended conformation, $\theta \approx 140^\circ$, arises stretching a folded conformation by increasing the Φ_1 and Φ_2 torsion angles to $130-170^\circ$. The distances between the erstwhile H-bonding components are a bit too large to accommodate the intramolecular H-bonding shown in the «ridge-tile» conformation, and the total steric energy increases exponentially as $\Phi_1 \approx \Phi_2 \rightarrow 170^\circ$. (e) The linear conformation, $\theta \approx 180^\circ$, leads to approximate co-planarity of the pyrromethenone rings by rotations of the Φ_1 and Φ_2 torsion angles to $\sim 180^\circ$. This conformation suffers from severe steric hindrance between the C_8 and C_{12} propionic acid groups. The conformations represented in (a), (b) and (e) are ≥ 12 kcal/mol higher in energy than the «ridge tile» conformer; conformer (d) is ≥ 5 kcal/mol higher energy than (c) — see ref. 26.

gen bonds, some intermolecular, some intramolecular, are formed, and the picture (Figure 4) is one of solvent (isopropylamine) bridging the propionic and

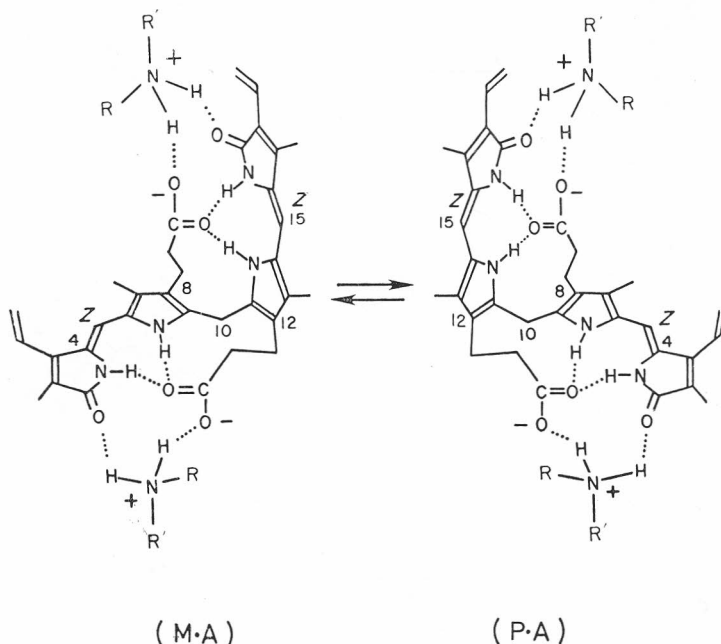


Figure 4. Interconverting, intramolecularly hydrogen-bonded diastereomeric conformers of bichromophoric amine bis salt complexes of bilirubin-IX α chiral amines (R and/or R' contains a chiral center). When R'=isopropyl and R=hydrogen that is H-bonded to $-\text{COO}^-$, the structures correspond to those found in the X-ray crystal structure of the bis-isopropylammonium salt of BR-IX (ref. 30). The **M·A** diastereomeric complex has left-handed (−) chirality of the two pyrromethenone chromophores; the **P·A** diastereomeric salt has right-handed (+) chirality.

pyrromethenone moieties. Even when solvent or polar groups insert into the hydrogen bonding matrix of the »ridge-tile« structures, the pigment seems to maintain a preference for a folded conformation, stabilized by varying degrees of inter and intramolecular hydrogen bonding. (A similar conclusion was reached for the bilirubin dianion,³¹ where the number of intramolecular hydrogen bonds is reduced, but the strength of the remaining hydrogen bonds increased.³² This structure is both striking and important because (i) the pigment adopts the folded, enantiomeric conformations and (ii) the amine salt linkage provides an insight into the structural basis for the ICDs of Table 3 and a clue as to how BR-IX might bind to serum albumin and other proteins via, e.g., lysine or arginine amine residues.^{18,19}

The origin of the induced optical activity may thus be understood simply in terms of non-equimolar concentrations of the diastereomeric salt (**M·A** and **P·A**) formed between a chiral amine, or amine residue (**A**) of the protein and the enantiomeric structures (**M** and **P**) of Figure 1. The position of the conformational equilibrium (**M** \rightleftharpoons **P**) for the uncomplexed mirror images **M** and **P** is expected to be unperturbed from $K_{\text{eq}} = 1$ to first approximation,

neglecting anisotropic solvation effects. However, the conformational equilibrium ($\mathbf{M} \cdot \mathbf{A} \rightleftharpoons \mathbf{P} \cdot \mathbf{A}$) between the heteroassociation complexes of \mathbf{M} and \mathbf{P} with a chiral amine (\mathbf{A}) is expected to have $K_{\text{eq}} \neq 1$ because the complexes are diastereomeric, with different ΔG_f° . Thus, the net concentration of \mathbf{M} species [\mathbf{M}] + ($\mathbf{M} \cdot \mathbf{A}$)] will not be equal to that of the \mathbf{P} species [\mathbf{P}] + ($\mathbf{P} \cdot \mathbf{A}$)], and the solutions will exhibit optical activity for the pigment. Optically active solutes that bind tightly to and are highly selective in forming heteroassociation complexes with one bilirubin enantiomer are expected to generate the most intense optical activity. This has already been noted for serum albumins, with which BR-IX exhibits intense ICD Cotton effects (CEs) typically in the range $|\Delta\epsilon| \approx 20\text{--}50 \text{ l} \cdot \text{mol}^{-1} \cdot \text{cm}^{-1}$,⁸ although values as high as $|\Delta\epsilon| \approx 250$ have been published.¹² However, chiral complexation agents or moieties that either do not have a large affinity constant or exhibit little selectivity for one enantiomer generate weaker optical activity for BR-IX, with ICD CEs in the range $|\Delta\epsilon|$ less than one order of magnitude.

The Importance of Carboxy Groups for Pigment Conformation in Chiral Complexation

In the case of protein binding we assume that stereocontrol of the pigment conformational equilibrium (Figure 1.) is affected primarily by amine salt formation to the bilirubin carboxyl groups. In general, chiral recognition involves, at a minimum, an acid-base equilibrium of the type shown in non-stoichiometric eqs. [1] and [2]. When \mathbf{A} is a chiral amine or amine residue, e. g., lysine,¹⁸ $K_{\text{eq}}^1 \neq K_{\text{eq}}^2$.



(Although the bis-salt complex is shown, the minimal (mono-salt) complexes would serve equally well in the arguments that follow.) The binding equilibria for ephedrine and ψ -ephedrine follow the expected solvent dependency, with non-polar solvents supporting tightly bound ion-pair salt structures and polar hydrogen-bonding solvents facilitating dissociation. Thus, in solvents such as methanol or dimethylsulfoxide, the ICD CEs are expected²¹ and found (Table IV) to be much weaker than in benzene or chloroform.

There are at least two fundamental considerations for interpreting the amine-pigment ICD data. In the first, the extremely large ICD bisignate CEs, which are characteristic of molecular exciton systems^{8,33} cannot arise simply from dissymmetric perturbation by (amine) solvation effects on an erstwhile achiral pigment. Rather, the bichromophoric pigment probably adopts predominantly one unique chiral conformation under the influence of the ephedrine. In the second, we see the ICD as originating from a BR-IX salt (complex) with the chiral amine (Figures 1. and 4.), as governed by eqs. [1] and [2]. As such, the CEs should be sensitive to the relative concentration of acid and base, exactly as observed (Tables I and II), with $\Delta\epsilon^{\text{max}}$ increasing sharply as the amine: pigment ratio increases from 10:1 to 100:1, more gradually from 100:1 to 1,000:1, and nearly levelling off between 1,000:1 and 5,000:1. The data follow the expectations of typical mass law type

TABLE 4. Circular Dichroism (CD) and Ultraviolet-Visible (UV) Spectral Data for $3.4 \times 10^{-5} \text{ M}$ Solutions of Bilirubin-IX α and $3.4 \times 10^{-2} \text{ M}$ Optically Active Amino-alcohols at 21°C.^a

Amino-alcohol	Solvent ^b	Time(h) ^c	CD			UV
			$\Delta\epsilon_{\text{max}}(\lambda_1)$	λ_2 at $\Delta\epsilon=0$	$\Delta\epsilon_{\text{max}}(\lambda_3)$	$\epsilon_{\text{max}}(\lambda, \text{nm})$
(-)- ψ -Ephedrine (-)-2(R)-Methylamino- 1(R)-phenyl-1-propanol	C ₆ H ₆	0.5	-40.8 (410)	437	+58.7 (470)	59,000 (460)
		24	-39.3 (410)	436	+52.0 (470)	58,700 (460)
	CHCl ₃	0.5	-37.4 (413)	433	+51.3 (465)	58,000 (450)
		24	-36.5 (410)	433	+49.6 (464)	56,900 (450)
	CH ₃ CN	0.5	-20.7 (395)	412	+50.0 (441)	61,000 (442)
		24	-19.9 (394)	411	+49.9 (441)	60,000 (442)
	CH ₃ OH	0.5	- 1.4 (405)	426	+ 1.9 (450)	57,000 (452)
		24	- 1.1 (404)	420	+ 2.1 (450)	56,000 (452)
(CH ₃) ₂ SO	0.5	\ll 0.1	---	\ll 0.1	59,000 (460)	
	24	\ll 0.1	---	\ll 0.1	57,800 (458)	
(+) - Ephedrine (+)-2(R)-Methylamino- 1(S)-phenyl-1-propanol	C ₆ H ₆	0.5	-45.8 (467)	485	+23.8 (495)	57,100 (464)
		24	-45.8 (465)	484	+23.2 (495)	55,100 (464)
	CHCl ₃	0.5	-58.6 (434)	462	+60.9 (485)	55,100 (456)
		24	-55.1 (435)	463	+58.8 (485)	52,100 (454)
	CH ₃ CN	0.5	-15.3 (448)	470	+ 8.0 (484)	60,000 (445)
		24	-15.5 (449)	471	+ 7.1 (484)	59,600 (447)
	CH ₃ OH	0.5	- 2.2 (404)	421	+ 5.2 (458)	61,000 (452)
		24	- 2.2 (406)	424	+ 4.2 (458)	60,000 (454)
(CH ₃) ₂ SO	0.5	\ll 0.1	---	\ll 0.1	59,200 (460)	
	24	\ll 0.1	---	\ll 0.1	58,000 (459)	
(-)-N-Methyl- ψ -ephedrine, (+)-2(R)-Dimethylamino- 1(R)-phenyl-1-propanol	C ₆ H ₆	0.5	- 1.5 (400)	435	+ 1.0 (464)	54,000 (460)
		24	- 1.5 (400)	435	+ 0.8 (464)	52,300 (458)
	CHCl ₃	0.5	- 1.8 (403)	427	+ 2.2 (456)	61,000 (456)
		24	- 1.1 (404)	428	+ 1.5 (452)	61,200 (455)
	CH ₃ CN	0.5	- 3.0 (400)	421	+ 3.0 (447)	58,600 (440)
		24	- 3.2 (400)	420	+ 3.3 (447)	58,000 (442)
	CH ₃ OH	0.5	- 1.6 (400)	420	+ 2.0 (442)	64,000 (453)
		24	- 1.1 (400)	422	+ 1.5 (446)	60,300 (454)
(CH ₃) ₂ SO	0.5	\ll 0.1	---	\ll 0.1	66,000 (461)	
	24	\ll 0.1	---	\ll 0.1	64,300 (461)	
(+) - Norephedrine (+)-2(R)-Amino- 1(S)-phenyl-1-propanol	C ₆ H ₆	0.5	-46.3 (420)	441	+56.9 (475)	55,000 (460)
		24	-35.1 (419)	440	+49.8 (474)	51,000 (460)
	CHCl ₃	0.5	-42.9 (415)	436	+56.6 (467)	63,000 (460)
		24	-45.0 (415)	436	+58.9 (466)	60,000 (459)
	CH ₃ CN	0.5	-32.0 (405)	427	+42.2 (459)	59,000 (444)
		24	-32.2 (405)	427	+42.3 (459)	56,000 (443)
	CH ₃ OH	0.5	- 2.4 (405)	429	+ 3.2 (459)	61,800 (452)
		24	- 2.3 (405)	429	+ 2.6 (456)	61,000 (452)
(CH ₃) ₂ SO	0.5	\ll 0.1	---	\ll 0.1	66,000 (460)	
	24	\ll 0.1	---	\ll 0.1	65,000 (460)	

^a 1,000:1 amino-alcohol:bilirubin molar ratio.

^b C₆H₆:benzene.

^c Spectra run 0.5 hours and 24 hours after solution preparation.

^d An overlapping long wavelength (-), short wavelength (-) bisignate exciton CD gives rise to trisignate CEs with short wavelength components at (0.5 h): C₆H₆, +26.1 (410), $\Delta\epsilon=0$ at 430 nm; CHCl₃, +1.7 (385), $\Delta\epsilon=0$ at 396 nm; CH₃CN, +9.9 (402), $\Delta\epsilon=0$ at 419 nm. After 24 h: C₆H₆, +26.1 (413), $\Delta\epsilon=0$ at 430 nm; CHCl₃, +2.9 (385), $\Delta\epsilon=0$ at 397 nm; CH₃CN, +9.4 (401), $\Delta\epsilon=0$ at 419 nm.

behavior for equations [1] and [2], where more of the CD-active complex is formed at the higher amine: pigment ratios as the equilibrium is shifted increasingly to the right.

Consistent with the view that salt-formation is an essential component for the production of intense pigment ICDs, the dimethyl ester of BR-IX (BR-IX DME) at best exhibits only extremely weak ICDs with ephedrine (Table V). Since BR-IX DME is not known to form amine salt complexes

TABLE 5. Circular Dichroism (CD) and Ultraviolet-Visible (UV) Spectral Data for 1.7×10^{-5} M Solutions of Bilirubin-IX α , its Analogs and 1.7×10^{-2} M (+)-Ephedrine at 21°C in chloroform.^a (Pigment:Ephedrine Ratio is 1:51000)

Pigment	Time (h) ^b	CD			UV	
		$\epsilon_{\max}(\lambda_1)$	λ_2 at $\Delta\epsilon=0$	$\Delta\epsilon_{\max}(\lambda_3)$	$\epsilon_{\max}(\lambda_{nm})$	
Bilirubin-IX α	0.5	-61.9 (437)	467	+60.1 (485)	53,700	454
	24	-54.7 (438)	467	+53.5 (490)	52,000	454
Mesobilirubin-XIII α	0.5	-75.8 (402)	420	+100.2 (448)	59,000	435
	24	-73.3 (401)	420	+99.1 (448)	50,000	436
Mesobilirubin-IV α	0.5	≤ 0.1	---	≤ 0.1	30,000	380
	24	≤ 0.1	---	≤ 0.1	25,000	380
Bilirubin-IX α Dimethyl Ester	0.5	≤ 0.1	---	≤ 0.1	61,000	420
	24	≤ 0.1	---	≤ 0.1	58,000	416
Xanthobilirubinic Acid	0.5	≤ 0.1	---	≤ 0.1	30,000	415
	24	≤ 0.1	---	≤ 0.1	29,000	414

^a Ethanol-free, stabilized with 1% n-hexane.

^b Spectra run 0.5 hours and 24 hours after preparing solutions.

but it can adopt folded conformations similar to those of Figure 1. (and molecular mechanics calculations^{26,27} confirm them as global minima), the absence of an ICD points to minimal enantioselection in the absence of amine salt formation. It is tempting to view low intensity ICDs as originating from solvation effects akin to those observed for BR-IX DME in ethyl (S)-(-)-lactate ($\Delta\epsilon_{410}^{\max} = -3$, $\Delta\epsilon_{430}^{\max} = +2.5$) and (-)-(2R,3R)-butanediol ($\Delta\epsilon_{405}^{\max} = -0.4$, $\Delta\epsilon_{430}^{\max} = +0.8$).³⁴ Thus, in the overall scheme, the conformational equilibria depicted in Figures 1. and 4., hence the relative stability of the complexes **M·A** and **P·A**, is determined by the enantioselectivity expressed by the equilibrium constants for the acid-base equilibrium reactions of eqs. [1] and [2].

Since intense ICDs appear to be crucially dependent on a heteroassociation complexation, eqs. [1] and [2], that require carboxylic acid functional groups

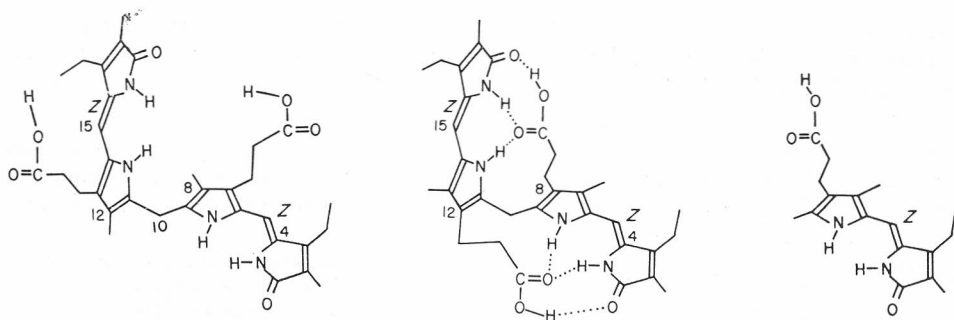


Figure 5. (From left to right) (4Z,15Z)-mesobilirubin-IV α (MBR-IV), which has its propionic acid groups located at sites from which intramolecular H-bonding to the opposing pyrromethenone units is rendered sterically impossible; (4Z,15Z)-mesobilirubin-XIII α (MBR-XIII), which is a structural isomer of MBR-IV that is capable of intramolecular H-bonding; and (4Z)-xanthobilirubinic acid, the parent mono-pyrromethenone of MBR-XIII.

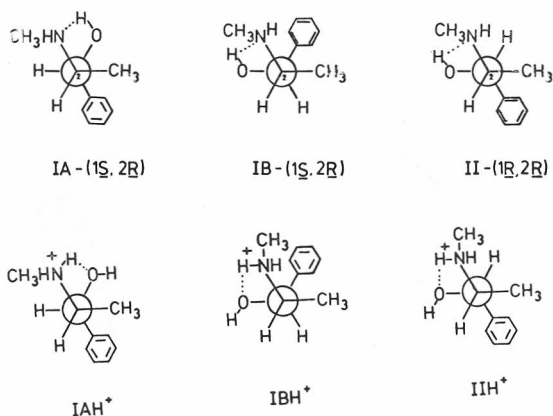
in the pigment, ICDs might therefore be expected to be seen with bilirubin analogs, e.g., the symmetric mesobilirubins-XIII α and IV α (MBR-XIII and MBR-IV, respectively), and even with the mono-pyrromethenone xanthobilirubinic acid (XBR) (Figure 5.). However, no significant ICD CEs can be detected for XBR in the presence of (+)-ephedrine (Table V). Yet it is clear that some sort of complexation interaction (salt formation) must take place between the amine and XBR because the pigment is extremely insoluble and will not dissolve in chloroform solvent at the indicated concentration in the absence of the amine. One might conclude, therefore, that significant pigment ICD is characteristic of the bichromophoric and not monochromophoric pigments. However MBR-IV which like XBR is also insoluble in chloroform in the absence of the amine, similarly gave only vanishingly small CEs (Table V). Although MBR-IV can adopt a folded conformation, which molecular mechanics calculations identifies as an energy minimum conformation,^{26,27} it cannot assume the intramolecularly H-bonded, folded conformations of Figures 1. and 3. because its propionic acid groups, no longer located at C₈ and C₁₂, are too distant. Apparently the location of the propionic acid groups is also a crucial factor for the production of significant pigment ICDs. In marked contrast strong, well-defined bisignate CEs are seen for MBR-XIII, which like BR-IX is capable of adopting and prefers to assume the chiral conformations of Figures 1. and 3. In summary, intense ICDs originating from bilirubin pigments in the presence of ephedrine requires propionic acid functional groups at C₈ and C₁₂ (which stabilize the folded conformations) in the bichromophoric pigment and is not due uniquely to other forces, e.g., micellar, electrostatic or π -interactions in the heteroassociation complexation of eqs. [1] and [2].

Molecular Models for Cooperative Binding

When it is highly enantioselective, the complexation process would appear to involve more than merely an acid-base equilibrium. As noted above, the data of Table III reveal that other aspects of molecular structure play a role, including steric factors and complementarity in the binding process.

For example, the strong preferential selectivity of (*R*)- β -phenylisopropylamines for **P** and not **M** or vice-versa, appear to involve dipole-dipole interactions or van der Waals attractions between the amine's π -electron rich aromatic ring and the pigment's pyrromethenone chromophores, in addition to hydrogen-bonding in the amine salt complex **M**·**A** or **P**·**A**.

Previous NMR studies of ephedrine and ψ -ephedrine favor conformations **IA** (and to a lesser extent **IB** and **II**, respectively, in which the OH and the CH_3NH groups are gauche and intramolecularly hydrogen-bonded $\text{N}\cdots\text{H}-\text{O}$).⁵⁵ These appear to predominate in both chloroform and dimethylsulfoxide solvents. Their ammonium ions, too, apparently adopt the corresponding gauche conformations, ephedrine: **IAH**⁺ (mainly), **IBH**⁺ and ψ -ephedrine: **IIH**⁺, with intramolecular hydrogen bonding coming from the methylammonium ion, $\text{N}-\text{H}\cdots\text{O}-\text{H}$. Assuming that conformers of the type **I** and **II** are important



in enantio-selective binding to BR-IX (either **M** or **P**, Figure 1), one might conclude from the intense CEs of Table IV that the bilirubin salt for **P** and (–)- ψ -ephedrine conformer **II** [to give **P**·**A** (Figure 1), where **AH**⁺ is **IIH**⁺] is more stable than that from **M** and **H** [giving **M**·**A**, where **AH**⁺ is **HH**⁺]. With (+)-ephedrine conformer, **IA**, the predominant BR-IX salt would also be **P**·**A** (where **AH**⁺ of Figure 1. is **IAH**⁺). It is important to note that the orientation of the phenyl group, which was previously²¹ noted to be very important in generating large CEs, is *trans* to the methylamino group in the preferred conformations of (–)- ψ -ephedrine, (+)-ephedrine and their salts.

Possible cooperative binding models for the complexes with (–)- ψ -ephedrine and (+)-ephedrine are illustrated in Figure 6. The models invoke a π -stacking arrangement of the phenyl and pyrromethenone group similar to that found recently in the ephedrinium mandelate salts³⁶ and in β -arylethylammonium carboxylate salts in Rebek's models for molecular recognition.³⁷ Presumably the (*R*)- β -phenylisopropylamines adopt complexes akin to those of Figure 6a. and c., yielding a predominance of the **P**·**A** diastereomer and thus intense, positive chirality bisignate CEs, cf. Table III, However, unlike (*R*)-*N,N*-dimethyl- β -isopropylamine (Table III), (2*R*)-*N*-methyl- ψ -ephedrine does not induce the large CE magnitudes that are seen for ψ -ephedrine in CHCl_3 ,

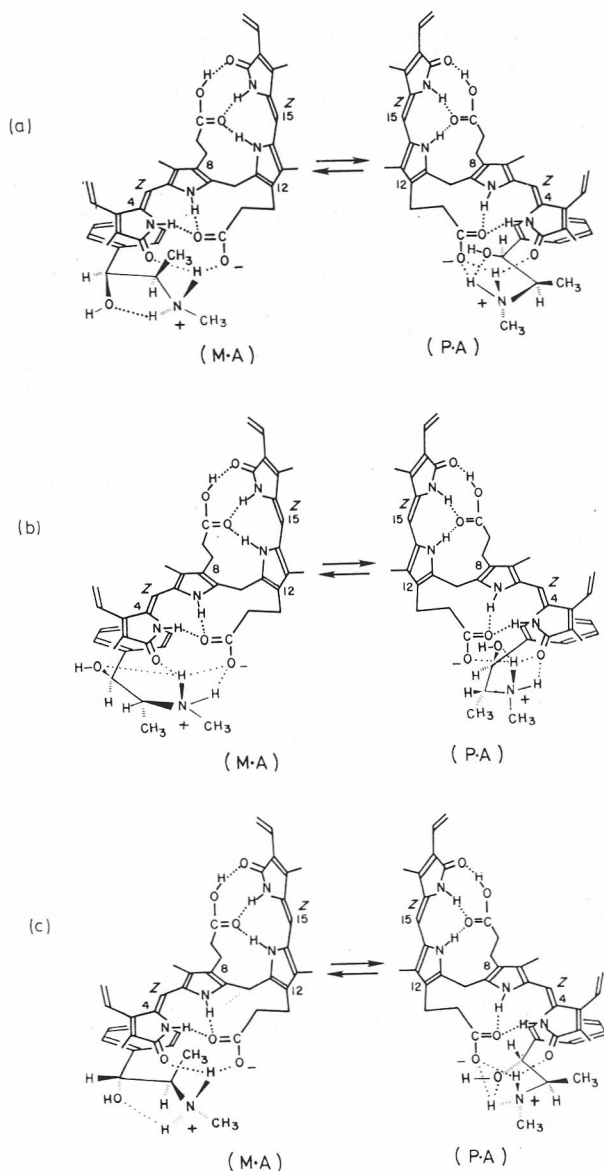


Figure 6. (a) Diastereomeric heteroassociation complexes of BR-IX with conformer **IA** of (1*S*,2*R*)-(+)-ephedrine showing multiple point binding through pi-stacking and the amine salt linkage found in the X-ray crystal structure of the BR-IX isopropylamine complex (ref. 30). Only the monosalt is shown for clarity of representation. The diastereomeric complex on the left (**M·A**) requires the amine component to adopt a conformation with an unfavorable steric interaction between the amine α -methyl and β -phenyl groups (and BR-IX). This complex is expected to be less stable than the complex on the right (**P·A**). (b) Diastereomeric heteroassociation complexes of BR-IX with the **IB** conformer of (+)-ephedrine. The **M·A** conformer is less sterically crowded than that on the right (**P·A**). (c) Diastereomeric heteroassociation complexes of conformer **II** of (1*R*,2*R*)-(–)-*ψ*-ephedrine. The **P·A** conformation on the right is the less sterically crowded than the **M·A**.

(Table IV). Although the bisignate CD retains the same signed order of CEs, the intensities coming from the N-methyl- ψ -ephedrine complex are more than an order of magnitude weaker. Apparently intramolecular hydrogen bonding in the N-methylated ephedrine unit appears to diminish greatly the ability to form a salt with bilirubin, e. g., K_1 and K_2 of eqs. [1] and [2] are reduced. Such intramolecular hydrogen bonding by the ephedrine OH group orients the two methyl groups of the dimethylaminomoiety away from the molecule, thus adding steric hindrance to salt formation with BR-IX. Such salts would be weak ion pairs. This problem is not encountered in norephedrine, which has no N-methyl groups, and it behaves similarly to ephedrine in inducing an intense bisignate CD for BR-IX (Table IV).

With ephedrine but not ψ -ephedrine, and BR-IX in non-polar solvents (Figure 2., Table IV), a smaller bisignate ICD of opposite signed order overlaps with the predominant long wavelength positive, short wavelength negative major ICD. This component may be seen as originating from a small presence of rotamer **IB** in equilibrium with **IA**, yielding additional new **M·A** and **P·A** complexes where **AH⁺** (Figure 1.) is **IBH⁺**. The cooperative binding models of Figure 6b. would suggest, on the basis of steric effects, that the **M·A** salt would predominate over the **P·A**, opposite to that deduced for **IA** and consistent with overlapping bisignate CEs of opposite signed sequence.

Using the binding models of Figure 6., one might predict that O-methylation of (+)-ephedrine (**IA** and **IB**) should destabilize **P·A** (Figure 6a. and 6b.) by imposing severe steric hindrance in the hydrogenbonding matrix (replace O—H by O—CH₃). The consequence of O-methylation should thus be a bisignate CD for BR-IX complexed with (+)-ephedrine methyl ether strongly characteristic of **M·A**. This in fact is observed (Table 6.): a sign inversion with intense CEs, long wavelength negative, short wavelength positive. O-methylation of (—)- ψ -ephedrine (**II**), in contrast, does not invert the signs (cf. Tables IV and VI). This is consistent with the binding model (Figure 6c.), wherein the ψ -ephedrine OH groups are pointed away from the hydrogen bonding matrix in both **M·A** and **P·A** and thus do not present the same steric hindrance to complexation as observed above for (+)-ephedrine. There is, nevertheless, an apparent stabilization of **P·A** (**AH⁺** = **IIH⁺**) because the CE magnitudes are significantly larger for the methyl ether than for the parent ψ -ephedrine. The reason for this is presently unclear.

Bisignate ICDs, Exciton Coupling and Absolute Configuration

Bisignate CEs are characteristic of the ICD spectra of the specific bichromophoric molecules studied here: Br-IX and MBR-XIII, and to a lesser extent, MBR-IV and BR-IX dimethyl ester. CD spectra with two oppositely-signed CEs straddling high intensity (large ϵ) UV-visible bands are typical of excited state (dipole) interaction, called exciton coupling, between two proximal chromophores with little orbital overlap.³³ Here, the component pyromethenone chromophores of the bichromophoric rubinoid pigments have strongly allowed long wavelength electronic transitions ($\epsilon_{410}^{\max} \sim 30,000$) but only a small interchromophoric orbital overlap in the folded conformation ($\sim 100^\circ$ dihedral angle) of Figure 3c. The orbital overlap increases and the exciton chirality decreases as the interplanar (dihedral) angle between the

pyrromethenone chromophores tends toward 0° (planar helical) or toward 180° (linear extended). In the latter case, the long wavelength UV-visible band of the pigment should tend to sharpen and red-shift as the transition probability to the higher energy exciton state decreases; in the latter case, the band should tend to sharpen and blue shift as the transition probability to the lower energy exciton state decreases.^{33,38} Concomitant changes would attend the CD spectra, with the shape moving from bisignate with roughly equal intensities to monosignate, with most of the intensity in one of CD couplets.³⁴ Numerous examples have been recognized,²⁰ including that of bilirubin-IV α .⁸ Thus, the bisignate CD curves (Figure 1) with comparably intense $\Delta\epsilon$ values for each member of the exciton couplet, offer a compelling argument for the folded conformation.

In the intramolecular exciton³⁸ represented by the folded conformation, the pyrromethenones interact through their locally excited states by resonance splitting [electrostatic interaction of the local transition moment dipoles (Figure 1.)]. The pyrromethenone-pyrromethenone intramolecular exciton splitting interaction produces two long wavelength transitions in the ordinary (UV-visible) spectrum and two corresponding bands in the CD spectrum.³⁹ One band is higher in energy and one is lower in energy, with the separation dependent on the strength and relative orientation of the pyrromethenone electric dipole transition moments.¹⁰ As seen in their UV-visible spectra, the two electronic transitions overlap to give the characteristically broadened absorption bands of bilirubins. As seen in their CD spectra, however, the two exciton transitions are always oppositely signed, as predicted by theory,³³ and thus give rise to bisignate CEs. In contrast to UV-VIS absorption bands, which may show only slight broadening when the exciton splitting energy is small, when two oppositely-signed curves overlap in the CD, there is considerable cancellation in the region between the band centers with the net result that the observed bisignate CE maxima are displaced from the actual locations of the (uncombined) CD transitions³⁹ and typically are seen to flank the corresponding UV-VIS band(s). This is amply illustrated by the induced CD and UV-VIS spectra of Figure 2. where the CEs are characteristic of exciton systems.³³

Bisignate CDs might also arise in bichromophoric bilirubins if each pyrromethenone acted independently to produce CEs of opposite signs. The optical activity could thus be attributed to asymmetric perturbation or induced dissymmetry of the chromophore — through the action of a chiral ligation ligating agent. However, in agreement with Blauer⁷ we tend to believe that this mechanism is unimportant for explaining the observed large CEs of bilirubin-protein complexes because: (i) the monochromophore molecular analog xanthobilirubic acid shows only a weak monosignate CD, and (ii) the CD couplets for the bichromophoric molecules are always of opposite sign, as required by the exciton model. If the chromophores were acting independently, one should expect to find monosignate CDs but never strong bisignate CDs.

Exciton coupling theory provides a way to assign the absolute configuration, *e. g.*, folded conformations akin to either **M** · **A** or **P** · **A** (Figures 1. and 4.), of the pigment in the predominant heteroassociation complex. The handedness or screw sense that the electronic transition moments of the

TABLE 6. Circular Dichroism (CD) and Ultraviolet-Visible (UV) Spectral Data for 3.4×10^{-5} M Solutions of Bilirubin-IX α and 3.4×10^{-2} M Optically Active Ephedrine Methyl Ethers at 21°C.^a

Amine	Solvent ^b	Time(h) ^c	CD			UV
			$\Delta\epsilon_{\max}(\lambda_1)$	λ_2 at $\Delta\epsilon=0$	$\Delta\epsilon_{\max}(\lambda_3)$	$\epsilon_{\max}(\lambda, \text{nm})$
<u>(+)-Ephedrine Methyl Ether, (+)-2(R)-Methyl-amino-1(S)-phenyl-1-propanol methyl ether</u>	C ₆ H ₆	0.5	+109.2 (411)	434	-150.2 (463)	55,000 (461)
		24	+ 92.0 (411)	434	-129.7 (464)	54,000 (461)
	CHCl ₃	0.5	+ 95.1 (408)	430	-131.7 (459)	57,000 (455)
		24	+ 94.4 (408)	430	-129.8 (459)	55,600 (455)
	CH ₃ CN	0.5	+ 49.4 (407)	429	- 67.9 (458)	59,000 (450)
		24	+ 50.2 (406)	429	- 69.8 (457)	57,900 (449)
	CH ₃ OH	0.5	+ 4.7 (402)	428	- 5.1 (456)	61,500 (451)
		24	+ 5.5 (404)	430	- 7.1 (453)	60,000 (451)
	(CH ₃) ₂ SO	0.5	+ 3.8 (412)	434	- 5.5 (464)	62,000 (462)
		24	+ 3.5 (413)	434	- 5.1 (462)	58,000 (461)
<u>(-)-ψ-Ephedrine Methyl Ether, (-)-2(R)-Methyl-amino-1(R)-phenyl-1-propanol methyl ether</u>	C ₆ H ₆	0.5	-142.9 (418)	436	+209.7 (469)	55,100 (458)
		24	-106.2 (418)	436	+160.2 (469)	59,000 (458)
	CHCl ₃	0.5	- 80.9 (409)	431	+111.6 (459)	51,200 (452)
		24	- 84.1 (410)	432	+113.6 (460)	51,000 (452)
	CH ₃ CN	0.5	- 61.8 (406)	429	+ 86.7 (458)	63,000 (451)
		24	- 60.4 (406)	429	+ 87.1 (458)	62,000 (450)
	CH ₃ OH	0.5	- 6.2 (408)	428	+ 8.8 (457)	64,000 (450)
		24	- 6.3 (407)	428	+ 7.9 (457)	63,000 (450)
	(CH ₃) ₂ SO	0.5	- 4.28 (416)	434	+ 6.65 (457)	61,000 (457)
		24	- 3.82 (412)	434	+ 5.57 (460)	59,400 (457)

^a 1,000:1 amine:bilirubin molar ratio.

^b C₆H₆:benzene.

^c Spectra run 0.5 hours and 24 hours after solution preparation.

coupled pyrromethenone chromophores make with each other correlates with signed order of the bisignate CD CEs.³⁹ A right-handed screw sense (positive chirality) of the transition moment leads to a (+) longer wavelength CE followed by a (-) shorter wavelength CE. For a left-handed screw sense (negative chirality) the CE signs are inverted: (-) at the longer wavelength and (+) at the shorter wavelength component of the bisignate CE. Since the direction of the electric dipole transition moment in the pyrromethenone chromophore has been calculated in theoretical studies¹⁰ to lie along the longitudinal axis of the planar conjugated π -system, the exciton model can predict the CE signs of the structurally well-defined diastereomers, such as **M** · **A** and **P** · **A**, as well as the enantiomers **M** and **P**. In those folded conformations, the relative orientations of the two pyrromethenone electric dipole

moments constitute a left-handed chirality for $\mathbf{M} \cdot \mathbf{A}$ and \mathbf{M} and a right-handed chirality for $\mathbf{P} \cdot \mathbf{A}$ and \mathbf{P} (with or without hydrogen bonding). Thus, theory predicts a predominance of the right-handed diastereomeric complex, e. g., $\mathbf{P} \cdot \mathbf{A}$ (or its folded analog of Figure 3c.) for solutions of bilirubin in the presence of (—)- ψ -ephedrine since the induced bisignate CDs show a long wavelength (+) CE followed by a short wavelength (—) CE (Figure 2.). Similarly, the $\mathbf{P} \cdot \mathbf{A}$ complex predominates in solutions of bilirubin with (+)-ephedrine.

Just as the absolute configuration can be assigned by exciton coupling theory, so can it be used to calculate the magnitudes of the CEs for enantiomers \mathbf{M} and \mathbf{P} and, by rough analogy, the CEs of the diastereomeric complexes $\mathbf{M} \cdot \mathbf{A}$ and $\mathbf{P} \cdot \mathbf{A}$. Using the formalism of Harada and Nakanishi,³³ we calculated maximum $\Delta\epsilon$ values of approximately +260 and —190 for the long and short wavelength exciton components, respectively, as seen in the theoretical CD curve of \mathbf{P} -helicity folded conformer.³⁶ With these calculated values as approximate standards for 100% diastereomerically pure complexes, the maximum experimental $\Delta\epsilon$ value (+60 at 470 nm) for BR-IX · (—)- ψ -ephedrine in benzene indicates an ~20% diastereomeric excess of the complex corresponding to $\mathbf{P} \cdot \mathbf{A}$.

Relevance to Albumin Binding

The binding of BR-IX to albumin and other proteins is an important facet of pigment transport and excretion;¹⁻⁵ yet, the nature of the binding and the structure of the bound pigment remain incompletely understood. The inference of the current work is (i) that the bilirubin species are bound to albumin (and other proteins) via salt linkages to protonated amine residues at the binding site, e. g., lysine^{18,40} and (ii) that complementary π -stacking binding interactions⁴¹ between the pyromethenone π -systems and nearby aromatic residues facilitates tight binding. Blauer and his coworkers⁷ have provided considerable insight into the structure of the bound pigment and its ICD by considering several possible conformations for the bound BR-IX.¹² Helical conformations with dissymmetric, twisted pyromethenone chromophores of fixed chirality, similar to the urobilins,⁴² were considered likely at first.⁴³ Subsequently, the dissymmetric (local) chromophore model was viewed as a less satisfactory explanation than the current model involving exciton interaction between the two pyromethenone chromophores held in a dissymmetric orientation.^{7,12} Using an exciton analysis, various conformations that might reproduce the CD data were considered:¹² (i) a porphyrin-like conformation (corresponding to $|\Phi_1| \simeq |\Phi_2| \simeq 0^\circ$, (ii) left and right-handed skew conformations akin to the lock-washer type helical molecular dissymmetry of the urobilins⁴² corresponding to $|\Phi_1| \simeq |\Phi_2| \simeq 10-20^\circ$, and (iii) extended conformations with »the largest possible distance between the chromophores« (corresponding approximately to $|\Phi_1| \simeq |\Phi_2| \simeq 140-180^\circ$) (see Figures 3a., b. and d, respectively). A dissymmetric extended conformation appeared to give the best fit in the data analysis. Later, a more refined analysis¹⁰ indicated the likelihood of a right-handed helical conformation for BR-IX bound to human serum albumin at neutral or higher pH [corresponding to $(\Phi_1 + \Phi_2 \simeq 30^\circ)$. Although recently an extended conformation ($\Phi_1 \simeq$

$\approx \Phi_2 \approx 140^\circ$) was proposed,¹¹ the current investigation points to the importance of the folded conformations of bilirubin salts ($|\Phi_1| \approx |\Phi_2| \approx 60\text{--}110^\circ$) of Figures 1. and 4. for the bound pigments. The folded conformations offer a consistent picture of the bound pigment as judged from (i) steric energy considerations^{26,27} that point to limited rotational flexibility about C₁₀, (ii) resonance Raman work that equates the conformation with the folded conformation deduced by NMR for BR-IX and BR-IX DME in DMSO,²⁹ (iii) complexation studies with amine binding models²¹ that point to a correlation between high degrees of enantioselectivity for hydrogen-bonded salt bridging and ancillary π -stacking, and (iv) earlier probes of the albumin-bilirubin binding site^{5,18,19,40} that reveal the importance of the lysine 240 residue and the likely involvement of tyrosine and histidine residues. A detailed conformational analysis and theoretical treatment of the pigment, including insights from molecular mechanics calculations, that relates conformation and torsion angles Φ_1 and Φ_2 to dihedral angle Θ and exciton coupling CD is currently under investigation.

CONCLUDING REMARKS

Bilirubin forms amine salt complexes with ephedrine. The binding constants, determined by an analysis of pigment UV spectral shifts and Hill plots giving good linearity, are ~ 200 for (+)-ephedrine and ~ 800 for (+)-ephedrine methyl ether. BR-IX and related rubins with propionic acid ($-\text{CH}_2\text{CH}_2\text{CO}_2\text{H}$) or propionate ($-\text{CH}_2\text{CH}_2\text{CO}_2^-$) groups located at C-8 and C-12 tend to adopt either of two intramolecularly hydrogen-bonded enantiomeric conformations (Figure 1.) and as such may be viewed as racemic mixtures of interconverting mirror image structures. Enantioselective binding to chiral amines, such as the ephedrine of the study, generates diastereomeric salt complexes (Figures 1. and 4.) in which one diastereomer (**M**·**A** or **P**·**A**) is favored over the other. As a consequence, BR-IX solutions become optically active and exhibit bisignate CD CEs, the intensity of which depends on the binding constant and enantioselectivity. The very large bisignate CEs previously characteristic only of albumin and other protein complexes with BR-IX can be detected for certain β -arylethylamines, which must also bind to BR-IX with a high degree of enantioselectivity.

We suggest that the amine binding enantioselectivity is high because of complementarity at the binding sites, e. g., amine salt formation stabilized by π -stacking of the amine aromatic residue to a pigment pyrromethenone. Some of the same complementarity is potentially available at the albumin binding site, which is known to contain a lysine amine residue as well as aromatic residues, e. g., tyrosine and histidine. Other potentially important complementary binding elements from ephedrine might include ancillary H-bonding from hydroxyl groups, but on the basis of the ephedrine model, these contributions would appear to be of greater importance for dictating ephedrine rotamers than for direct participation in BR-IX enantio-selection.

Conformations such as **M** and **P** (Figure 1.) and **M**·**A** and **P**·**A** appear to be essential in understanding the origin of the intense bisignate ICD CEs. For those bichromophoric pigments (MBR-IV, BR-IX dimethyl ester) that cannot or do not adopt them give only extremely weak ICD CEs in the

presence of chiral amines. Consequently, although we view all the bichromophoric pigments of this study potential molecular excitons, only BR-IX and MBR-XIII show bisignate ICD data characteristic of exciton systems wherein the two chromophores are held in the well defined geometry (Figures 1., 3c., 4. and 5.) necessary for near optimal orientation (interplanar pyrromethenone-pyrromethene skew angle of $\sim 100^\circ$) of their relevant electric dipole transition moments.

Acknowledgement. — We thank the National Institutes of Health (HD-17779) for generous support of this work and J.-Y. An for preliminary ICD studies with (—)-ephedrine.

EXPERIMENTAL DETAILS

Bilirubin-IX α (BR-IX) contained less than 5% of the III α and XIII α isomers, as obtained from Porphyrin Products and determined by high performance liquid chromatography.⁴⁴ Bilirubin-IX α dimethyl ester (BR-IX DME) was isolated following reaction of BR-IX with diazomethane, as described previously.⁴⁵ Mesobilirubins IV α and XIII α (MBR-IV and MBR-XIII) and xanthobilirubinic acid (XBR) were prepared by total synthesis.^{46,47} The amines used in this work were obtained from Aldrich: (1*S*,2*R*)-(+)-ephedrine $[\alpha]_D^{21} + 41^\circ$ (c 5, 1M HCl), (1*R*,2*R*)-(—)- ψ -ephedrine $[\alpha]_D^{20} - 49^\circ$ (c 0.6, ethanol), (1*S*,2*R*)-(+)-norephedrine $[\alpha]_D^{20} 40^\circ$ (c 7, 1 M HCl) R-(—)-2-aminobutanol $[\alpha]_D + 9.8^\circ$ (neat), S-(+)-des-N-methyl-desoxyephedrine $[\alpha]_D + 36^\circ$ (neat), S-(+)-desoxyephedrine $[\alpha]_D + 18^\circ$ (H₂O) for HCl salt; Norse Laboratories: R-(—)-2-aminobutane $[\alpha]_D - 7.5^\circ$ (neat); and Fluka: R-(—)-alaninol $[\alpha]_D^{20} - 22 \pm 2^\circ$ (c 2, ethanol), R-(—)-1-amino-2-propanol $[\alpha]_D^{20} - 18 \pm 1^\circ$ (c 1.8, H₂O) and R-(—)-phenyl-1,2-ethanediol $[\alpha]_D^{20} - 39 \pm 1^\circ$ (c 2, acetone). The organic solvents used were spectral grade. Solutions were prepared by dissolving the pigment in a freshly prepared amine solution, and the spectral data were accumulated within 30 minutes and after 24 hours of preparation. All circular dichroism spectra were recorded on a JASCO J-600 spectropolarimeter or on a JASCO J-40 spectropolarimeter equipped with a photoelastic modulator, and all UV-visible spectra were run on a Cary 219 spectrophotometer.

(+)-(1*S*,2*R*)-Ephedrine Methyl Ether

According to previously published methods,^{48,49} ammonia (150 mL) was distilled and condensed in a 250 mL 3-N round bottom flask, cooked in a dry ice-acetone bath an equipped with a dry ice condenser, addition funnel and mechanical stirrer. Pieces of sodium (0.80 g, 0.035 g-atom) were added, followed by (+)-(1*S*,2*R*)-ephedrine (5.0 g, 0.030 mmole) in 50 mL of ether. Then 4.30 g (0.030 mmole) of iodo-methane was added, and the solution was allowed to come to room temperature by evaporation of the ammonia. The residue was filtered, and the solid material was washed with ether (2 \times 20 mL). Evaporation of the ether solution gave a colorless oil, 3.30 g. The desired product was separated from N-methylated and O,N-dimethylated by-products on a column of silica gel (50 cm long \times 4.5 cm diam.) using CHCl₃ : CH₃OH : conc NH₄OH (8 : 1 : 0.1 vol/vol/vol). The pure methyl ether eluted first to afford 1.70 g (31%) as an oil. It had $[\alpha]_D^{23} = + 53^\circ$ (CHCl₃); IR (film) ν : 3340 (w), 3040 (m), 2980 (s), 2940, 1380 (m), 1120 (s), 770, 710 (s) cm⁻¹; UV (CH₃OH) $\epsilon_{257}^{\max} = 122$ ¹H-NMR (CDCl₃) δ : 0.98 (3H, d, $J = 7$ Hz), 2.32 (3H, s), 3.25 (3H, s), 4.10 (1H, d, $J = 7$ Hz), 7.28 (5H, s) ppm.

(—)-(1*R*,2*R*)- ψ -Ephedrine Methyl Ether

This material was prepared as above from (—)- ψ -ephedrine in 30% yield. It had $[\alpha]_D = - 68.3^\circ$ (CHCl₃); IR (film) ν : 3350 (w), 3020 (w), 2950 (s), 1460 (s), 1380 (m), 1100 (s), 770, 710 (s) cm⁻¹; UV (CH₃OH) $\epsilon_{256}^{\max} = 126$; ¹H-NMR (CDCl₃) δ : 0.80 (3H, d, $J = 7$ Hz), 2.42 (3H, s), 3.17 (3H, s), 3.85 (1H, d, $J = 7$ Hz), 7.30 (5H, s) ppm.

REFERENCES

1. D. A. Lightner and A. F. McDonagh, *Accounts Chem. Res.* **17** (1984) 417.
2. For leading references see J. D. Ostrow, ed., *Bile Pigments and Jaundice*, Marcel Dekker, Inc., New York, 1986.
3. A. F. McDonagh and D. A. Lightner, *Pediatrics* **75** (1985) 443.
4. A. F. McDonagh, in *The Porphyrins* (Dolphin, D., ed.) Vol. VI, Academic Press, New York, 1979, pp. 293–491.
5. R. Brodersen, in *Bilirubin* (Heirwegh, K. P. M. and Brown, S. S., eds.) Vol. I, CRC Press, Boca Raton, FL, 1982, pp 75–123.
6. R. Brodersen, *CRC Crit. Rev. Clin. Lab. Sci.*, **11** (1979) 305.
7. G. Blauer, *Isr. J. Chem.* **23** (1983) 201.
8. D. A. Lightner, M. Reisinger, and G. L. Landen, *J. Biol. Chem.* **261** (1986) 6034.
9. J. Jacobsen and R. Brodersen, *J. Biol. Chem.* **258** (1983) 6319.
10. G. Blauer and G. Wagnière, *J. Amer. Chem. Soc.* **97** (1975) 1949.
11. R. B. Lauffer, A. C. Vincent, S. Padinanabhan, and T. J. Meade, *J. Amer. Chem. Soc.* **109** (1987) 2216.
12. G. Blauer, D. Harmatz, and J. Snir, *Biochem. Biophys. Acta* **278** (1972) 68.
13. R. Bonnett, J. E. Davies, M. B. Hursthouse, and G. M. Sheldrick, *Proc. R. Soc. London Ser. B* **202** (1978) 249.
14. G. LaBas, A. Allegret, Y. Mouguen, C. DeRango, and M. Bailly, *Acta Crystallogr.* **B36** (1980) 3007.
15. For leading references see D. Kaplan and G. Navon, *Isr. J. Chem.* **23** (1983) 177.
16. D. A. Lightner, in *Bilirubin* (Heirwegh, K. P. M., and Brown, S. B., eds.) Vol I, CRC Press, Boca Raton, FL, 1982, pp 1–58.
17. N. Blanckaert, K. P. M. Heirwegh, and Z. Zaman, *Biochem. J.* **164** (1977) 229.
18. C. Jacobsen, *Biochem. J.* **171** (1978) 453.
19. C. Jacobsen, *Eur. J. Biochem.* **27** (1972) 513.
20. D. A. Lightner and J. Y. An, *Tetrahedron* **43** (1987) 4287.
21. D. A. Lightner, J. Y. An, and Y. M. Pu, *Archives Biochem. Biophys.* **262** (1988) 543.
22. R. Brodersen, in *Bile Pigments and Jaundice* (Ostrow, J. D., ed.), Marcel Dekker, Inc, New York, 1986, pp 157–181.
23. W. H. Pirkle and D. J. Hoover, *Topics in Stereochemistry* (Allinger, N. L., Eliel, E. L., and Wilen, S. H., eds.) Vol. **13**, J. Wiley, NY, 1982, pp 263–331.
24. G. R. Weisman, in *Asymmetric Synthesis* (Morrison, J. D., ed.) Vol. **1**, Academic Press, NY, (1983), pp 153.
25. D. A. Lightner, J. K. Gawroński, and K. Gawrońska, *J. Amer. Chem. Soc.* **107** (1985) 2456.
26. H. Falk and N. Müller, *Monatsh. Chem.* **112** (1982) 1325; *Tetrahedron* **39** (1983) 1875.
27. D. A. Lightner, R. Person, and T. Polonski, unpublished data.
28. D. Kaplan and G. Navon, *Biochem. J.* **201** (1982) 605.
29. Y. Z. Hsieh and M. D. Morris, *J. Amer. Chem. Soc.* **110** (1988) 62.
30. A. Mugnoli, P. Manitto, and D. Monti, *Acta Crystallogr. Sect. C* **C38** (1983) 1287. The torsion angles Φ_1 and $\Phi_2 \approx 61^\circ$ for the bis-isopropylammonium salt, and the pyrromethenone-pyrromethenone interplanar (dihedral) angle is 97° .
31. D. A. Lightner, J.-S. Ma, and X.-X. Wu, *Spectroscopy Lett.* **19** (1986) 311.
32. M. Meot-Ner, *J. Amer. Chem. Soc.* **110** (1988) 3854.
33. For a recent review see e.g., N. Harada and K. Nakanishi, *Circular Dichroic Spectroscopy-Exciton Coupling in Organic Stereochemistry*, University Science Books, Mill Valley, CA (1983).
34. A. R. Holzwarth, E. Langer, H. Lehner, and K. Schaffner, *Photochem. Photobiol.* **32** (1980) 17.
35. P. S. Portoghese, *J. Med. Chem.* **10** (1967) 1057.
36. W. P. Zingg, E. M. Arnett, A. T. McPhail, A. A. Bothner-By, and W. R. Gilkerson, *J. Amer. Chem. Soc.* **110** (1988) 1565.

37. J. Rebek, Jr., B. Askew, P. Ballester, and A. Costero, *J. Amer. Chem. Soc.* **110** (1988) 923.
38. M. Kasha, H. R. Rawls, and M. A. El-Bayoumi, *Pure Appl. Chem.* **32** (1965) 371.
39. D. A. Lightner, J. K. Gawroński, and W. M. D. Wijekoon, *J. Amer. Chem. Soc.* **109** (1987) 6354.
40. Guanidation of the lysine residues of HSA results in greatly decreased binding of BR-IX. N. H. Martin, *J. Amer. Chem. Soc.* **71** (1947) 1230.
41. P. Bothorel and J. P. Desmazes, *Biochim. Biophys. Acta* **365** (1974) 181.
42. A. Moscowitz, W. C. Krieger, I. T. Kay, G. Skewes, and S. Bruckenstein *Proc. Natl. Acad. Sci. (U. S.)* **52** (1964) 1190.
43. G. Blauer and T. King, *Biochem. Biophys. Res. Commun.* **31** (1968) 678.
44. A. F. McDonagh, L. A. Palma, F. R. Trull, and D. A. Lightner, *J. Amer. Chem. Soc.* **104** (1982) 6860.
45. D. A. Lightner and F. R. Trull, *Spectroscopy Lett.* **16** (1983) 785.
46. D. A. Lightner, J.-S. Ma, R. W. Franklin, and G. L. Landen, *J. Heterocyclic Chem.* **21** (1983) 139.
47. F. R. Trull, R. W. Franklin, and D. A. Lightner, *J. Heterocyclic Chem.* **24** (1987) 1573.
48. F. D. Cazer, A. R. Kausar, K. S. Kumar, M. N. Inbasekaran, and D. T. Witniak, *J. Radiolabelled Cpds. Radiopharm.* **XIX(4)** (1982) 585.
49. C. Kashima, K. Harada, and Y. Omote, *Can. J. Chem.* **63** (1985) 288.

SAŽETAK

Intramolekulsko ekscitonsko sprezanje i cirkularni dikroizam heteroasocijacijskog kompleksa bilirubin-efedrin. Stereokemijski model za vezanje proteina

Yu-Ming Pu i David A. Lightner

Bikromorfni (4Z, 15Z)-bilirubin-IX_a citotoksični, žuto-narančasti pigment žutice, nastoji zauzeti jednu od dvije enantiomerne, konformacije karakterizirane intramolekulskom vodikovom vezom, koje su u dinamičkoj ravnoteži u otopini. U prisustvu optički aktivnih amino-alkohola, osobito efedrina, otopina pigmenta pokazuje intenzivan dvo-predznačni cirkularni dikroizam u području bilirubinske UV-vidljive apsorpcijske vrpce u dugovalnom području. Najintenzivniji Cottonovi efekti, $|\Delta\epsilon| \rightarrow 200$, inducirani su O-metil-efedrinom nadilaze čak i one koje pokazuju kompleksi bilirubina sa serum-albuminom i drugim proteinima. Poput serum-albumina i drugih proteina, i optički aktivni amino-alkoholi djeluju kao kiralni templati (kalupi) inducirajući asimetričnu transformaciju bilirubina, čiji inducirani dvo-predznačni Cottonov efekt potječe od ekscitonskog cijepanja njegovog dvokomponentnog pirometenonskog kromofora. Pretpostavlja se da amini služe kao agensi za kiralno molekulsko prepoznavanje, dajući diastereomerne soli s pigmentom. Komplementarno djelovanje β -arila i susjednih hidroksilnih i metoksilnih skupina omogućava dodatni uvid u vezne sile značajne za proces vezanja bilirubina na proteine.